Journal of Materials Chemistry A

COMMUNICATION

View Article Online
View Journal | View Issue

Cite this: J. Mater. Chem. A, 2017, 5, 16134

Received 24th January 2017
Accepted 20th March 2017

DOI: 10.1039/c7ta00833c

rsc.li/materials-a

Pine-branch-like TiO_2 nanofibrous membrane for high efficiency strong corrosive emulsion separation†

Yuanyuan Zhang,‡ Yuee Chen,‡ Lanlan Hou, Fengyun Guo, Jingchong Liu, Shanshan Qiu, Yue Xu, Nü Wang* and Yong Zhao*

Strong corrosive emulsion sewage must be properly treated because it is not only very harmful to the environment, but also an enormous waste of chemical resources. Here we fabricated a pine-branch-like TiO_2 nanofibrous membrane *via* an electrospinning and hydrothermal process. Besides neutral emulsions, the obtained membrane could separate various highly corrosive acidic (pH < 0), basic (pH > 14), and salty oil-in-water emulsions with efficiencies higher than 99% without extra force assistance, which is highly promising for aquatic environment protection as well as resource recycling.

The ever-increasing emissions of oily effluent deriving from textile, printing, leather and metal finishing industrial processes, and from daily life seriously threaten the ecosystem and the health of people's lives.[1,2] Effective separation of oily wastewater, especially surfactant stabilized emulsions with a dispersed droplet size less than 20 μm is urgently desired and has become a tough worldwide challenge.[3–5] Emulsified oil/water mixtures composed of complex components are more difficult to deal with because surfactant is amphiphilic with water and oil, which results in multiple molecular interactions.[6] Traditional emulsion separation techniques, such as electrochemical treatment,[7] centrifugation,[8,9] gravity separation,[10] ultrasonic separation,[11] air flotation,[12] coagulation[13] and biological treatment,[14] are usually of low efficiency and high energy consumption, and sometimes even bring secondary pollution.

In the last decade, membrane technology has been considered as one of the most efficient methods for oily water treatment because it has many advantages, including a high separation efficiency, low energy consumption and relatively simple operation.[15] Specially, membranes with special wetting properties and suitable pore sizes attract immense attention and are widely applied in the field of emulsion separation.[16–20] Currently, the emulsion separation membrane materials are mainly classified into two categories, namely polymeric membranes and inorganic membranes (ceramics or metals). The polymer membranes have many merits such as easy processability, flexibility and tailorability.[21–23] Nevertheless, polymer membranes usually cannot tolerate organic solvent dissolution and incline to degradation in strong alkaline liquids, which are often encountered in industrial emulsions. Comparatively, inorganic separation membranes are of superior resistance to organic solvents, but so far most of the reported inorganic membranes, such as $Cu(OH)_2$,[4] SiO_2,[24] Co_3O_4,[25] *etc.* still cannot resist corrosion by a strong acid or base, which not only destroys the membranes, but also releases some environmental toxic substances like Cu^{2+} and Co^{4+}. Therefore, development of a high efficiency emulsion separation membrane that possesses good chemical stability to organic solvents and strong corrosive liquids is of significant importance but still a big challenge. Titanium dioxide (TiO_2) is an environmentally friendly semiconductive oxide material with a superior chemical stability, which has been widely used in photocatalysis,[26–29] coatings,[30] cosmetics[31,32] and even food additives approved by the FDA.[33] Moreover, TiO_2 has a unique photoinduced superhydrophilic property that endows it with an outstanding performance in self-cleaning coatings and functional interfacial materials with special wettability.[34,35] We have demonstrated that surface modified TiO_2 nanofiber membranes could be used for separating free oil and water and two-phase organic liquids.[36] But such a single structural nanofibrous membrane could not be applied for the separation of emulsions because the pore sizes interweaved by cross fibers are too large to intercept the emulsion droplets. In this respect, drought-enduring conifers give us inspiration in that the dense needle-like leaves of the pine branch could effectively reduce water evaporation but not hinder the transmission of light for photosynthesis.[37,38] This strategy suggests that a dense pine branch structure

Key Laboratory of Bioinspired Smart Interfacial Science and Technology of Ministry of Education, Beijing Key Laboratory of Bioinspired Energy Materials and Devices, School of Chemistry, Beihang University, Beijing 100191, China. E-mail: wangn@buaa.edu.cn; zhaoyong@buaa.edu.cn; Fax: +86-10-82317801

† Electronic supplementary information (ESI) available. See DOI: 10.1039/c7ta00833c

‡ These authors contributed equally to this work.

microporous membrane should feasibly intercept small size oil droplets in the emulsion while keeping a high flux for water.

Herein, we fabricated a pine-branch-like TiO_2 membrane with hairy nanorods on nanofiber structures. The membrane could separate various neutral and strong corrosive acidic (pH < 0), basic (pH > 14), and salty emulsions in a highly efficient manner. This versatile separation membrane should be of great promise for water cleaning and resource recovery.

Scheme 1 describes the fabrication and separation processes of the pine-branch-like TiO_2 nanofibrous membrane. Firstly, a poly (vinyl pyrrolidone) (PVP)/TiO_2 composite nanofibrous membrane was fabricated by an electrospinning technique. Then the electrospun membrane was calcined and turned into an anatase TiO_2 nanofibrous membrane. After a hydrothermal reaction, TiO_2 nanorods grew on the nanofibers and formed a pine-branch-like membrane. In comparison with a pristine TiO_2 nanofibrous membrane, the relatively larger pores of the hydrothermal treated crossed fibers were bestrewed nanorods, which largely decreased the pore sizes. Such a pine-branch-like structure could be used to separate an oil-in-water emulsion.

Morphologies of the TiO_2 membrane are shown in Fig. 1. The electrospun PVP/TiO_2 membrane were composed of non-woven nanofibers with an average diameter of 630 nm (Fig. 1a and d). After calcination, the diameter of the nanofibers evidently decreased to an average value of about 406 nm owing to the degradation of PVP (Fig. 1b, d and S1†). It is clear that the nanofibrous TiO_2 membrane is of large pore size, and is unable to separate emulsions according to a "size-sieving effect".[16] Inspired by the hierarchical pine branches structure in nature (Fig. 1g), a hydrothermal strategy was chosen to grow secondary structure on every single TiO_2 fiber to narrow the big holes. After the hydrothermal process, a dense layer of TiO_2 nanorods evenly deposited on the nanofibers, thereby forming a pine-branch-like TiO_2 membrane (Fig. 1c, e and f). A top view of the pine-branch-like TiO_2 membrane is presented in Fig. 1c and e at different magnifications, which shows a uniform hairy branch morphology. A high magnification cross-sectional morphology of a single fiber (Fig. 1f) demonstrates that the nanorods grew vertically along the fibers leading to the formation of hierarchical structures. The average lengths and diameters of the nanorods were 584.2 ± 6.3 nm and 76.0 ± 2.2 nm, respectively. In the hydrothermal process, the length and density of pine-branch-like TiO_2 nanorods increased with prolonging the reaction time and increasing the concentration of titanium butoxide (TBT) (Fig. S2 and S3†). When fixing the hydrothermal solution concentration in a volume ratio of deionized water/hydrochloric acid/TBT = 30/30/1.5 and a reaction temperature at 150 °C, a sparse layer of TiO_2 nanoparticles deposited on single smooth TiO_2 fibers during the first hour. When prolonging the reaction time from 2 h to 6 h, the nanoparticles grew to nanorods whose lengths increased from 247.6 ± 11.2 nm to 602.7 ± 10.5 nm, resulting in smaller pore sizes (Fig. S2†). Similarly, when fixing the hydrothermal reaction system at 150 °C and the reaction time for 4 h, but changing the TBT concentration in different volume ratios (deionized water/hydrochloric acid/TBT = 30/30/0.5, 30/30/1.0, 30/30/1.5, 30/30/2.0, 30/30/2.5 and 30/30/3.0), the nanorod lengths changed from 94.4 ± 9.3 nm to 811.7 ± 40.3 nm *via* adjusting the TBT concentrations (Fig. S3†). These results demonstrated that the morphology of the hierarchical membrane can be controlled by tuning the reaction time and TBT concentration. By comparing the different morphologies produced in various reaction conditions, a reaction time of 4 h, deionized water/hydrochloric acid/TBT = 30/30/0.5 (v/v/v) and a reaction temperature of 150 °C were selected as the proper conditions for an efficient oil-in-water emulsion separation on the basis of energy consumption and time saving. Meanwhile, we characterized the crystal forms of the membranes. From the XRD patterns in Fig. 1h, it can be seen that the diffraction peaks of a pine-branch-like membrane matched well with anatase (JCPDS 21:1272) and rutile TiO_2 (JCPDS 21:1276) (black line).[39,40] As a comparison, the peaks of a pristine calcined nanofiber membrane matched well with anatase (JCPDS 21:1272) (red line).[40]

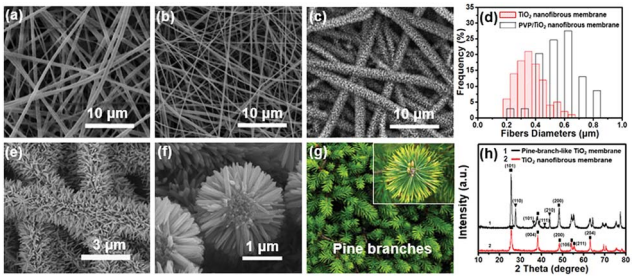

Fig. 1 SEM images of (a) electrospun PVP/TiO_2 nanofibrous membrane, (b) calcined TiO_2 membrane and (c) hydrothermal treated pine-branch-like TiO_2 membrane. (d) Fiber diameter distribution. (e) High magnification of the pine branch structures. (f) Cross sectional image shows that nanorods grew vertically along the fibers. (g) Photograph of leaves of a pine branch in nature. The as-fabricated membrane is very similar to natural pine branches. (h) XRD patterns of TiO_2 membranes during different stages.

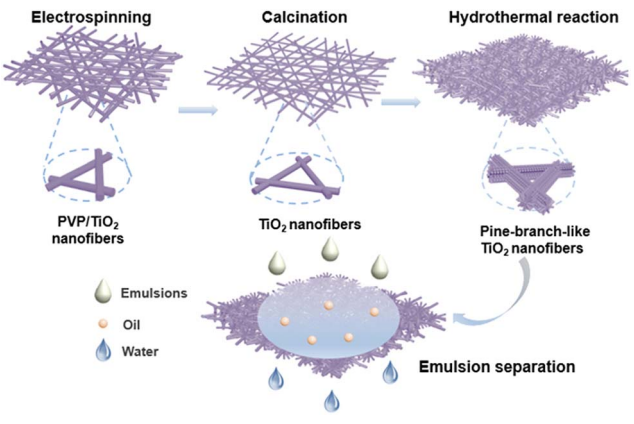

Scheme 1 Fabrication and separation processes of pine-branch-like TiO_2 membrane. Firstly, a composite PVP/TiO_2 membrane is prepared by an electrospinning technique. Then, the initial electrospun membrane is calcined to remove PVP and form TiO_2 nanofibrous membranes. Finally, the TiO_2 membrane is placed into an autoclave for hydrothermal reaction, and then a pine-branch-like TiO_2 membrane forms. The resultant pine-branch-like TiO_2 membrane is used for oil-in-water emulsion separation.

Besides a suitable pore sizes, the membrane's wetting behavior is also important for emulsion separation. The wettability properties of the membrane were characterized by measuring the water contact angles (WCAs) in air, oil contact angles (OCAs) and adhesion forces under water. WCAs on TiO_2 nanofibrous membranes and pine-branch-like TiO_2 membranes were nearly zero, while the underwater OCAs (gasoline) were 151.1 ± 0.5° and 158.8 ± 0.9°, respectively (Fig. 2a). The underwater OCAs of other oils on the membrane were further measured (Fig. 2b). Results showed that OCAs on the pine-branch-like TiO_2 membrane are all greater than 150° (petroleum ether (156.7 ± 0.8°), toluene (155.1 ± 0.6°), hexadecane (156.0 ± 1.2°), isooctane (153.5 ± 1.3°), gasoline (158.8 ± 0.9°) and diesel (153.5 ± 1.3°)), higher than those on bare TiO_2 nanofibrous membranes (petroleum ether (147.9 ± 2.9°), toluene (151.1 ± 1.6°), hexadecane (149.7 ± 3.0°), isooctane (149.1 ± 1.3°), gasoline (151.1 ± 0.5°) and diesel (146.4 ± 0.7°)). This difference mainly results from the higher roughness due to the formation of pine-branch-like structures.[41] This is because when the as-prepared membrane is underwater, the water is first trapped into the rough structure, forming a thin water layer and avoiding direct contact between oils and membrane surfaces. In other words, it formed an oil/water/solid three-phase interface,[21,42] and thus the oil droplet kept superoleophobic underwater. The pine-branch-like TiO_2 membrane also exhibited an extremely low oil-adhesion force whose value is nearly 0 μN for diesel (Fig. 2c) and 0.015 μN for toluene (Fig. 2d). The detail processes of a 4 μL droplet touching and leaving the membrane surface were recorded (Fig. S4†). The underwater superoleophobicity and extremely low adhesive property are greatly advantageous to the antifouling property of the membrane.[43]

It is well known that TiO_2 has been widely applied due to its photocatalytic property,[44] self-cleaning,[45] and photoinduced wettability change.[46] To examine the UV-induced wetting behavior of the pine-branch-like TiO_2 membrane, we compared the water spreading time before (Fig. 2e) and after (Fig. 2f) UV irradiation. The processes were recorded by a high-speed camera system. When a water droplet (4 μL) contacted the pine-branch-like TiO_2 membrane surface, it spread out within 207 ms without irradiation. After UV irradiation, the spread time is dramatically decreased to less than 70 ms. These results demonstrated that UV irradiation makes the TiO_2 membrane more superhydrophilic due to the UV-induced hydroxyl groups on the surface of the TiO_2 nano-needles,[34] which would increase the flux during subsequent emulsion separation.

Then the pine-branch-like TiO_2 membrane was used to test the emulsion separation performance (Fig. 3a). Tween-20-stabilized oil-in-water emulsions (oils include gasoline, diesel, isooctane, hexadecane, toluene, and petroleum ether) were poured onto the pine-branch-like TiO_2 membrane to realize separation driven solely by gravity. During the separation process, a water/solid interface would form and prevent the dispersed oil droplets contacting the membrane. The small oil droplets in the emulsion were captured by the TiO_2 needle-like structure and the size of the oil droplets would turn bigger due to the coalescence effect. Meanwhile, clear water flowed down and passed through the pine-branch-like TiO_2 membrane perfectly finishing a demulsification process.[47] Fig. 3b shows that the original emulsion is milky white with a clear Tyndall effect, while the filtrate is transparent without a Tyndall effect.

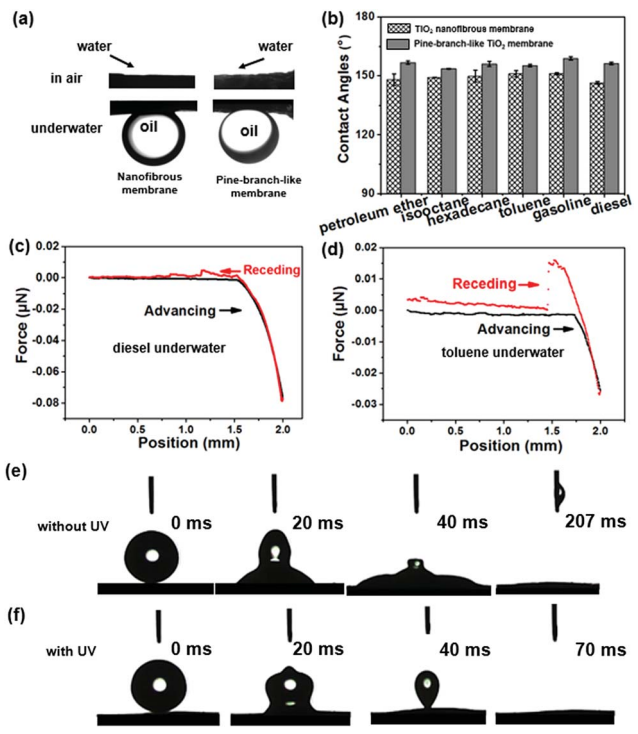

Fig. 2 Wettability characterization of membranes. (a) Water contact angle and underwater oil contact angle of a bare TiO_2 nanofibrous membrane (left) and a pine-branch-like TiO_2 membrane (right). (b) Statistics of underwater oil contact angles on two kinds of membranes. (c) and (d) Adhesion force curve of diesel and toluene on a pine-branch-like membrane. (e) and (f) Water spreading behavior of the pine-branch-like TiO_2 membrane before and after UV irradiation.

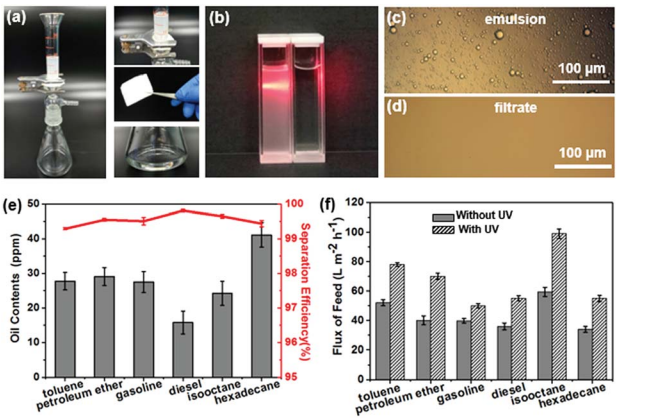

Fig. 3 (a) Set-up for oil-in-water emulsion separation. (b) Tyndall scattering phenomenon by using a red light to irradiate the gasoline-in-water emulsion (left) and filtrate (right). (c) and (d) Optical microscopy images of the gasoline-in-water emulsion and the filtrate. (e) Oil content and separation efficiency of various filtrates. (f) Flux of the membrane increases after UV irradiation.

Optical microscopy images of gasoline-in-water emulsions and filtrates are shown in Fig. 3c and d; dense oil droplets were seen in the feed emulsion whereas no droplets were observed in the filtrate. This indicated that the emulsion had been successfully separated. Dynamic light scattering (DLS) curves of six kinds of oil-in-water emulsions are shown in Fig. S5.† The DLS pattern indicates that the distribution of the oil droplets is in the range from 41.1 nm to 313.5 nm, proving that the pine-branch-like TiO_2 membrane can separate emulsions with dispersed droplet sizes in this range. The exact oil concentrations in the filtrates were measured by an infrared spectrometer oil content analyzer according to the infrared absorption spectra of oils. The separation efficiency is defined and calculated by the oil rejection coefficient R (%) before and after separation according to the following equation:

$$R = \left(1 - \frac{C_p}{C_o}\right) \times 100\% \quad (1)$$

where C_o and C_p are the oil concentration of the original oil/water emulsion and the collected oil concentration after separation, respectively. As shown in Fig. 3e, the oil contents in the filtrates were all below 45 ppm for oil-in-water emulsions (oils include petroleum ether 29.1 ± 2.6 ppm, toluene 27.8 ± 2.5 ppm, hexadecane 41.0 ± 2.3 ppm, isooctane 24.3 ± 3.5 ppm, gasoline 27.5 ± 3.0 ppm, and diesel 15.8 ± 3.3 ppm) and corresponding separation efficiencies all above 99% (petroleum ether (99.55% ± 0.04%), toluene (99.29% ± 0.03%), hexadecane (99.44% ± 0.09%), isooctane (99.65% ± 0.05%), gasoline (99.51% ± 0.11%), and diesel (99.81% ± 0.04%)). To testify the necessity of a secondary TiO_2 nano-needle structure construction, we also took an additional separation experiment using the TiO_2 nanofibrous membrane. The corresponding separation efficiencies were all less than 87%, which indicated that the TiO_2 nanofibrous membrane lacks separation ability (Fig. S6†). This means that the suitable pore sizes and superhydrophilicity/underwater superoleophobicity endow the membrane with an excellent separating capability. The flux of the TiO_2 membrane was calculated by measuring the time needed for a certain volumes of oil-in-water emulsions. The fluxes of the Tween-20 stabilized oil-in-water emulsions are in the range 36–59 L m^{-2} h^{-1} for various types of emulsion with different viscosities (Fig. 3f). Surprisingly, fluxes of filtrate under UV-irradiation have an evident increase in the range of 50–99 L m^{-2} h^{-1}. The obvious flux comparison between without UV and with UV mainly results from an UV-induced enhanced superwetting property (Fig. 2e, f).[34] Additionally, the antifouling performance of the pine-branch-like TiO_2 membrane was investigated (Fig. S7 and S8†). The stable flux and high separation efficiency indicated an outstanding recovery performance of the membrane.

Compared to a neutral emulsion, corrosive emulsions are also commonly encountered in chemical industries or labs. Therefore, the separating material must be stable in corrosive environments such as a strong acid, a strong alkali, or high concentration salt solutions. To test the anti-corrosion stability, pine-branch-like TiO_2 membranes were immersed in corrosive solutions for one week; it is seen (Fig. 4a) that the membranes still exhibited good superoleophobicity in 4.0 mol L^{-1} HCl (pH < 0), NaOH (pH > 14) and NaCl aqueous solutions. We also compared the morphology change before and after immersing in harsh environments; the results revealed that there were almost no changes before and after immersion (Fig. S9†). Furthermore, three kinds of corrosive emulsions made from gasoline and corresponding 4 mol L^{-1} HCL, NaOH, and NaCl aqueous solutions were prepared. The results showed that the emulsion separation efficiency remained above 99% (Fig. 4b), which indicates a good chemical stability against strong alkali, acid and salt conditions. Fig. 4c–e are three bottles of 4 mol L^{-1} acid, base, and salt corrosive emulsions and the corresponding filtrates. These results indicate that the pine-branch-like TiO_2 membrane has a good environmental stability and is a good candidate in corrosive industrial oil-contaminated water treatment.

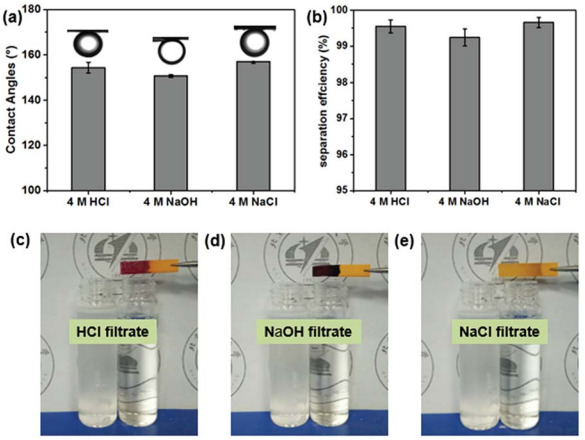

Fig. 4 Chemical stability of the pine-branch-like TiO_2 membrane. (a) Gasoline contact angles on pine-branch-like membrane in 4.0 mol L^{-1} HCl (pH < 0), NaOH (pH > 14), and NaCl aqueous solutions (pH = 7). (b) The separation efficiency of the pine-branch-like TiO_2 membrane for strong acid, basic, and salty emulsions. (c) Left: Gasoline-in-4 M HCl emulsion (pH < 0), right: pH test paper changes brownish red with 4 M HCl filtrate (pH < 0). (d) Left: Gasoline-in-4 M NaOH emulsion (pH > 14), right: pH test paper changes dark blue with 4 M NaOH filtrate (pH > 14). (e) Left: Gasoline-in-4 M NaCl emulsion (pH = 7), right: pH test paper remains yellow with 4 M NaCl filtrate (pH = 7).

Conclusions

A pine-branch-like TiO_2 membrane has been successfully prepared by electrospinning, calcination and hydrothermal reaction. The resultant membrane exhibits superhydrophilicity in air and superoleophobicity underwater, and the pine-branch-like structure endows suitable pore sizes for emulsion separation. Due to the strong chemical stability of TiO_2, the as-prepared membrane can be applied for separating emulsions in a harsh environment, such as strong acidic (pH < 0), basic (pH > 14) and salt solutions, with a relative high efficiency above 99%. This pine-branch-like TiO_2 membrane is expected to have promising applications in the wastewater treatment and resource recovery.

Acknowledgements

The authors acknowledge the NSFC (21433012, 21374001, 21134003, 2122309), 863 Program (2013AA032203), the National Youth Talent Support Program for New Century Excellent Talents in University of China, the Fundamental Research Funds for the Central Universities, the China Scholarship Council (201506025110) and the National Instrumentation Program (2013YQ120355)

Notes and references

1 Y. Yu, H. Chen, Y. Liu, V. S. J. Craig, C. Wang, L. H. Li and Y. Chen, *Adv. Mater. Interfaces*, 2015, **2**, 1400267.
2 T. Dong, G. Xu and F. Wang, *J. Hazard. Mater.*, 2015, **296**, 101.
3 M. A. Shannon, P. W. Bohn, M. Elimelech, J. G. Georgiadis, B. J. Marinas and A. M. Mayes, *Nature*, 2008, **452**, 301.
4 F. Zhang, W. B. Zhang, Z. Shi, D. Wang, J. Jin and L. Jiang, *Adv. Mater.*, 2013, **25**, 4192.
5 X. Lin, Y. Chen, N. Liu, Y. Cao, L. Xu, W. Zhang and L. Feng, *Nanoscale*, 2016, **8**, 8525.
6 Z. Shi, W. Zhang, F. Zhang, X. Liu, D. Wang, J. Jin and L. Jiang, *Adv. Mater.*, 2013, **25**, 2422.
7 P. Cañizares, F. Martínez, J. Lobato and M. A. Rodrigo, *J. Hazard. Mater.*, 2007, **145**, 233.
8 F. Ghasemi Naghdi and P. M. Schenk, *Bioresour. Technol.*, 2016, **218**, 428.
9 E. Turano, S. Curcio, M. G. De Paola, V. Calabrò and G. Iorio, *J. Membr. Sci.*, 2002, **209**, 519.
10 B. A. Grimes, *J. Dispersion Sci. Technol.*, 2012, **33**, 578.
11 L. J. Stack, P. A. Carney, H. B. Malone and T. K. Wessels, *Ultrason. Sonochem.*, 2005, **12**, 153.
12 A. A. Al-Shamrani, A. James and H. Xiao, *Water Res.*, 2002, **36**, 1503.
13 A. I. Zouboulis and A. Avranas, *Colloids Surf., A*, 2000, **172**, 153.
14 J. Liu, X. F. Huang, L. J. Lu, M. X. Li, J. C. Xu and H. P. Deng, *J. Hazard. Mater.*, 2011, **190**, 214.
15 M. Cheryan and N. Rajagopalan, *J. Membr. Sci.*, 1998, **151**, 13.
16 D. Liu, L. He, W. Lei, K. D. Klika, L. Kong and Y. Chen, *Adv. Mater. Interfaces*, 2015, **2**, 1500228.
17 N. Liu, M. Zhang, W. Zhang, Y. Cao, Y. Chen, X. Lin, L. Xu, C. Li, L. Feng and Y. Wei, *J. Mater. Chem. A*, 2015, **3**, 20113.
18 J. B. Fan, Y. Song, S. Wang, J. Meng, G. Yang, X. Guo, L. Feng and L. Jiang, *Adv. Funct. Mater.*, 2015, **25**, 5368.
19 M. Tao, L. Xue, F. Liu and L. Jiang, *Adv. Mater.*, 2014, **26**, 2943.
20 Y. Si, J. Yu, X. Tang, J. Ge and B. Ding, *Nat. Commun.*, 2014, **5**, 5802.
21 W. Zhang, Y. Zhu, X. Liu, D. Wang, J. Li, L. Jiang and J. Jin, *Angew. Chem., Int. Ed.*, 2014, **53**, 856.
22 Y. Hou, C. T. Duan, N. Zhao, H. Zhang, Y. P. Zhao, L. Chen, H. J. Dai and J. Xu, *Chin. J. Polym. Sci.*, 2016, **34**, 1234.
23 W. Zhang, Z. Shi, F. Zhang, X. Liu, J. Jin and L. Jiang, *Adv. Mater.*, 2013, **25**, 2071.
24 Y. Chen, N. Liu, Y. Cao, X. Lin, L. Xu, W. Zhang, Y. Wei and L. Feng, *Sci. Rep.*, 2016, **6**, 32540.
25 Y. Chen, N. Wang, F. Guo, L. Hou, J. Liu, J. Liu, Y. Xu, Y. Zhao and L. Jiang, *J. Mater. Chem. A*, 2016, **4**, 12014.
26 T. Ohno, K. Sarukawa, K. Tokieda and M. Matsumura, *J. Catal.*, 2001, **203**, 82.
27 S. Lakshmi, R. Renganathan and S. Fujita, *J. Photochem. Photobiol., A*, 1995, **88**, 163.
28 F. D. Fonzo, C. S. Casari, V. Russo, M. F. Brunella, A. L. Bassi and C. E. Bottani, *Nanotechnology*, 2009, **20**, 015604.
29 R. Zhang, X. Wang, J. Song, Y. Si, X. Zhuang, J. Yu and B. Ding, *J. Mater. Chem. A*, 2015, **3**, 22136.
30 M. Shalom, S. Dor, S. Rühle, L. Grinis and A. Zaban, *J. Phys. Chem. C*, 2009, **113**, 3895.
31 A. Jaroenworaluck, W. Sunsaneeyametha, N. Kosachan and R. Stevens, *Surf. Interface Anal.*, 2006, **38**, 473.
32 M. Auffan, M. Pedeutour, J. Rose, A. Masion, F. Ziarelli, D. Borschneck, C. Chaneac, C. Botta, P. Chaurand, J. Labille and J.-Y. Bottero, *Environ. Sci. Technol.*, 2010, **44**, 2689.
33 A. Weir, P. Westerhoff, L. Fabricius, K. Hristovski and N. von Goetz, *Environ. Sci. Technol.*, 2012, **46**, 2242.
34 K. Liu, M. Cao, A. Fujishima and L. Jiang, *Chem. Rev.*, 2014, **114**, 10044.
35 S. J. Gao, Z. Shi, W. B. Zhang, F. Zhang and J. Jin, *ACS Nano*, 2014, **8**, 6344.
36 L. Wang, Y. Zhao, Y. Tian and L. Jiang, *Angew. Chem., Int. Ed.*, 2015, **54**, 14732.
37 A. R. Studart and R. M. Erb, *Soft Matter*, 2014, **10**, 1284.
38 C. P. Souto, T. Kitzberger, M. P. Arbetman and A. C. Premoli, *New Phytol.*, 2015, **208**, 960.
39 H. Wang and Z. Guo, *Appl. Phys. Lett.*, 2014, **104**, 183703.
40 C. Sun, N. Wang, S. Zhou, X. Hu, S. Zhou and P. Chen, *Chem. Commun.*, 2008, 3293.
41 M. Liu, S. Wang, Z. Wei, Y. Song and L. Jiang, *Adv. Mater.*, 2009, **21**, 665.
42 X. Lin, Y. Chen, N. Liu, Y. Cao, L. Xu, W. Zhang and L. Feng, *Nanoscale*, 2016, **8**, 8525.
43 Y. Lai, J. Huang, Z. Cui, M. Ge, K. Q. Zhang, Z. Chen and L. Chi, *Small*, 2016, **12**, 2203.
44 J. C. Yu, J. G. Yu, W. K. Ho, Z. T. Jiang and L. Z. Zhang, *Chem. Mater.*, 2002, **14**, 3808.
45 Y. Paz, Z. Luo, L. Rabenberg and A. Heller, *J. Mater. Res.*, 1995, **10**, 2842.
46 R. D. Sun, A. Nakajima, A. Fujishima, T. Watanabe and K. Hashimoto, *J. Phys. Chem. B*, 2001, **105**, 1984.
47 J. Ge, J. Zhang, F. Wang, Z. Li, J. Yu and B. Ding, *J. Mater. Chem. A*, 2017, **5**, 497.

